GeoConvention 2015
GEOSCIENCE
new horizons
Telus Convention Centre • 4-8 May 2015 • Calgary, AB Canada

3D Finite Element Modeling of fault-slip triggering caused by pore-pressure changes

Arsalan Sattari and David W. Eaton
Department of Geoscience, University of Calgary

Summary

We present a 3D model using a widely used finite-element package, ABAQUS, to simulate activation of slip on a pre-existing fault due to an imposed perturbation in pore pressure on a subregion of the fault. The model inputs are 3 initial principal background stresses, elastic properties of the medium, coefficient of friction and geometry of the fault. Initial stresses are assigned according to Mohr Coulomb theory based on the assumption that the crust is in a critically stressed state. The calculation is shown to be stable, robust and consistent with Okada's analytical displacement calculation. Our results indicate that the fault rupture area is generally larger than the initially perturbed area. Moreover, the rupture area, and thus the earthquake magnitude, increases with the size of the perturbed area, irrespective of the overall fault dimensions. For example, our model predicts that a 2km by 2km area perturbed by 5 MPa pore pressure results in a magnitude 4.4 earthquake with 1 MPa (10 bar) of shear stress drop. For a given fault geometry and initial state, we interpret our calculations to represent an upper limit for earthquake magnitude, as the equivalent stress release could be achieved with a sequence of smaller events.

Introduction

Fluid injection can trigger earthquake activity on a nearby fault, either by increasing pore pressure or by poroelastic stress coupling between fractured lithologies and formation fluids (Ellsworth, 2013; Davies et al., 2013). A pore-pressure increase tends to reduce the effective normal stress on the fault plane and thus stimulates slip (Healy, 1968). Zoback (2012) showed that the majority of faults are subject to failure in response to a small perturbation in stress, relative to ambient stress levels. Keranen et al (2013) showed that pore pressure can travel tens of kilometers away from the injection site and can trigger slip on a fault with a pore-pressure perturbation as small as 0.07 MPa. Although the majority of injection-induced earthquakes are small in magnitude, the relatively high rates of induced seismicity significantly adds to seismic hazard in some areas (Ellsworth, 2013). Knowing the potential maximum magnitude of induced-earthquake is useful in seismic hazard assessment (McGarr, 2014); however it is highly dependent on factors including fluid-injection parameters, rheology and size of the fault. This study is motivated by the need to understand the dependency of maximum magnitude of induced earthquake to these factors.

Theory

In this study we aim to investigate the maximum earthquake magnitude that can be triggered by an increase of pore pressure around a fault. The examples presented here are confined to a strike-slip regime, but our method is applicable to any stress regime and fault geometry. According to Mohr-Coulomb failure criterion, fault slip occurs when the Mohr circle intersects or crosses the failure line

(Figure 1), where the slope of failure line is equal to coefficient of friction. Individual points on the Mohr circle represent the shear and normal stress for different fault orientations. A pore pressure (P_p) increase shifts the Mohr circle to left, and at the point of failure in critically stressed regime the maximum principal stress (σ_{max}) is given by (Zoback, 2010)

$$\sigma_{max} = \left[\sqrt{\mu^2 + 1} + \mu\right]^2 \sigma_{min} \quad ,$$

where σ_{min} is the minimum principal stress and μ is the coefficient of friction. For $\mu = 0.6$ the orientation of critically stressed fault deviates by 30 degrees from the maximum stress direction.

The vertical background stress S_v is defined by the pressure by the rocks lying above a particular depth. It is described by (Twiss and Moores, 2007) as

$$S_v = \int \rho_{Layer} g \quad dz$$

where ρ_{Layer} is density and g is gravitational acceleration. In this study, we use a stress state in which the vertical principal stress is the average of minimum and maximum principal horizontal stresses. Hence,

$$S_h = \frac{2}{1+\left[\sqrt{\mu^2+1}+\mu\right]^2} S_v.$$

Methodology

The finite element modeling in this study is calculated using ABAQUS. A 3D cubical model is used, covering a volume of 9km depth, 7km length and 9 km width. A 3km wide fault with a depth extent of 3 km is imposed in the middle of the model, starting at 3km depth. The coefficient of friction is set to 0.6. Young's modulus and Poisson's ratio are 80 MPa and 0.33, respectively. An average density of 2600 $\frac{kg}{m^3}$ is assumed for the entire model. All sides of the model except the surface have no degrees of freedom to move. At the top of the model, a free-surface boundary condition is applied. Hexahedral elements with full integration points (C3D8) are used. The dimensions of elements around the fault are about 20 m increasing to ~200 m at the sides. The average horizontal and vertical principal stresses are calculated on each element subject to the condition that the fault is critically stressed. Principal stresses are perturbed by a pore pressure increase in the target area. The first step in the procedure is to fix all the nodes and compute a reaction-force solution on each node, which equilibrates the initial stress condition. In the second step fault nodes are released to calculate the equilibrium point and slip on the fault. Convergence is validated by verifying a unique response subject to decreasing mesh size.

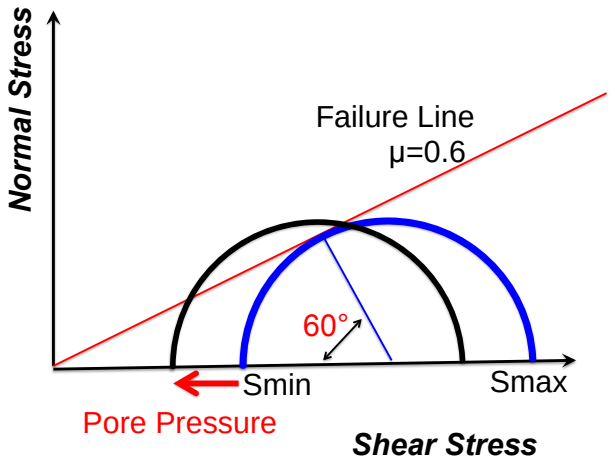

Figure 1 The blue Mohr circle is critically stressed at the tangent point with the failure line which makes a 60 degree angle with the shear stress axis. The black Mohr circle is shifted to the left to represent an increases in pore pressure. The part of black Mohr circle which is above the red line is in the unstable regime and is subject to failure.

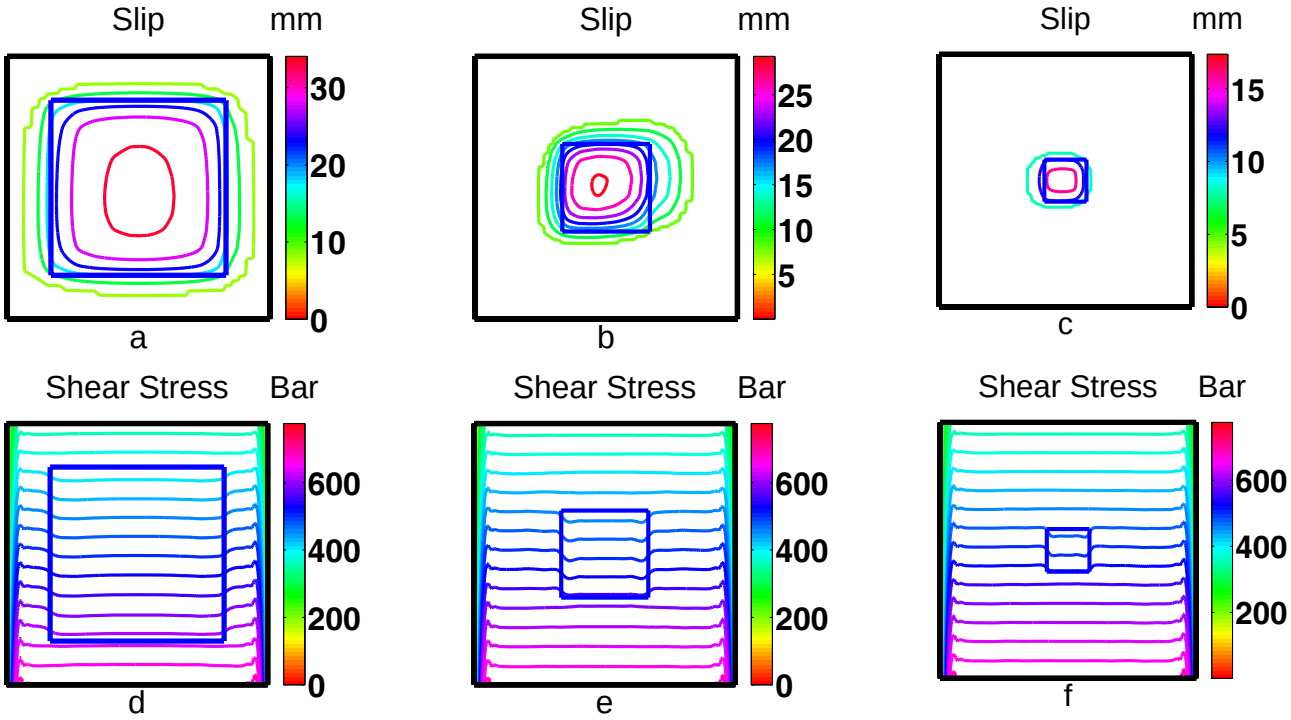

Figure 2 a), b) and c) Calculated slip contours in mm on a 3 km by 3 km fault plane. The initially perturbed region is indicated by the blue square. d), e) and f) Shear stress contours. Faults are located from 3km to 6km deep.

Results

Figure 2 shows slip pattern and shear stress contours for varying size of initially perturbed area (Table 1) on a 3km by 3km fault plane. Pore pressure perturbed volume is cubical and surrounds the fault plane symmetrically. The average slip increases proportionally to the perturbed volume. The slip is maximum in the middle of the pressure perturbed area and shrinks to zero as it propagates away. The rupture area is not bounded by the initially perturbed part of the fault and can be slightly larger. Asymmetry is displayed in slip and displacement pattern, which is due to changes in initial stress distribution applied by ABAQUS to reach equilibrium in the first step of the calculation. Asymmetry may also arise from the use of elements with different sizes around the fault. This issue can be resolved by using a smaller size of elements at the expense of a longer simulation time. A constant shear stress drop of ~1 MPa (10 bar) occurs for all three earthquakes, which is consistent with observed stress drops for induced earthquakes within our modelled depth range (e.g., Hough, 2014).

Okada (1985) calculated displacement inside a semi-infinite medium due to slip on a finite rectangular fault. The inputs of the model are two elastic parameters of medium, geometry and orientation of fault, strike-slip, dip-slip and tensile components of dislocation. Figure 3 shows a comparison between the finite element

Fault Size	Pore Pressure Change	Perturbed Area	Average Slip	Moment Magnitude	Shear Stress Drop
3km * 3km	5 MPa	0.5km *0.5km	12 mm (fig.1.a)	3.4	1 MPa (fig.1.d)
3km * 3km	5 MPa	1km * 1km	19 mm (fig.1.b)	3.9	1 MPa (fig.1.e)
3km * 3km	5 MPa	2km *2km	25 mm (fig.1.c)	4.4	1 MPa (fig.1.f)

Table 1 Model parameters and calculated results.

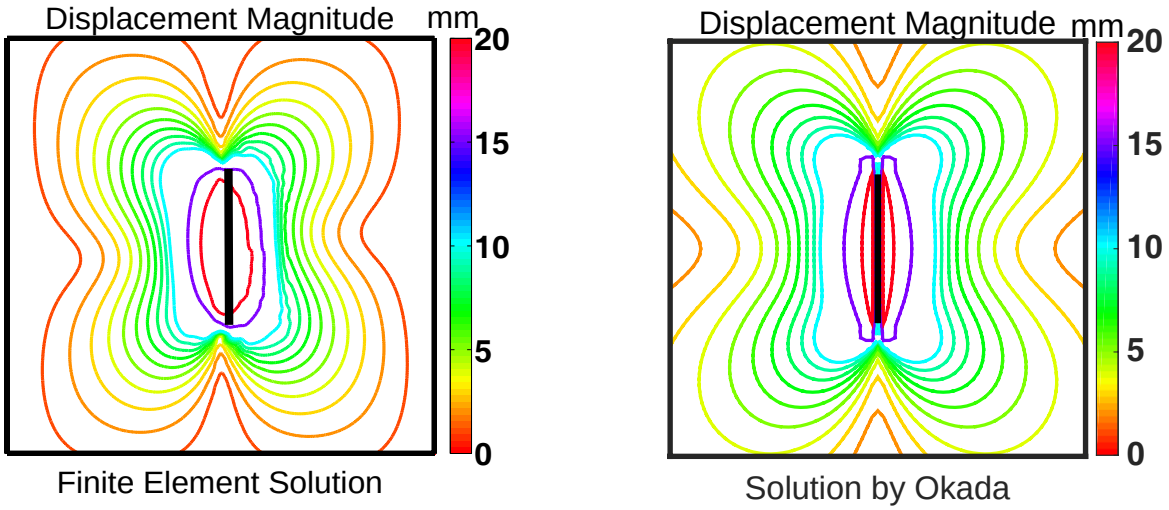

Figure 3 Both picures show a map veiw of 9km by 9km horizontal surface at 4.5 km depth. The black line presents a fault with 3km width and 3km length, starts at 3km depth. Left) Displacement magnitude of nodes resulted from an average of 4 cm slip according to finite element simulation. Right) Displacement magnitude resulted from 4cm uniform slip according to analythical solution by Okada (1985).

modelling result and Okada's model, verifying that our finite element model estimation is consistent with the theoretical solution.

Conclusions

The 3D finite element model that we proposed here is capable of simulating maximum slip on a fault plane in any faulting regime, which is useful in seismic hazard modeling. Also it can simulate the maximum magnitude of an earthquake due to pore-pressure increase on a fault. The model results are in agreement with Okada's theoretical solution of displacements. We find that the rupture area can be larger than the initially perturbed region. Moreover, slip increases as the perturbed area becomes larger. A 2km by 2km area, disturbed by 5 MPa pore pressure can trigger a 25mm average slip on the fault. Seismic moment (M_0) in dyne.cm is calculated by multiplying shear modulus (30 GPa), area of slip (~ 2.5km by 2.5km) and average slip. Therefore, moment magnitude 4.4 is calculated by using the formula given by (Hanks & Kanamori, 1979)

$$M = \frac{2}{3} log M_0 - 10.7.$$

Acknowledgments

This work was supported by a Collaborative Research and Development Grant from the Natural Sciences and Engineering Research Council of Canada. TransAlta Utilities and Nanometrics Inc. are also thanked for their support of this initiative.

References

Davies, R., G. Fouler, A. Bindley and P. Styles (2013), Induced seismicity and hydraulic fracturing for the recovery of hydrocarbons. Mar Petrol. Geol., **45**, 171-185.

Ellsworth, W. L. (2013), Injection-induced earthquakes. Science, **341**

Frohlich, C., and M. Brunt (2013), Two-year survey of earthquakes and injection/production wells in the Eagle Ford Shale, Texas, prior to the M 4.8 20 October 2011 earthquake. Earth Planet. Sci. Lett., **379**, 56-63.

Hanks, T. C., and H. Kanamori (1979), A moment-magnitude scale. J. Geophys. Res, **84**, 2348–2350.

Healy, J. H., W. W. Rubey, D. T. Griggs, and C. B. Raleigh (1968), The Denver earthquakes. Science, **161**, 1301-1310.

Hough, S. (2014). Shaking from injection-induced earthquakes in the central and eastern United States. Bull. Seismol. Soc. Am., **104**(5), 2619.

Keranen, K., H. Savage, G. Abers, and E. S. Cochran (2013), Potentially induced earthquake in Oklahoma, USA: links between wastewater injection and the 2011 M 5.7 earthquake sequence. Geology, **41**, 699-702.

McGarr, A. (2014) Maximum magnitude earthquake induced by fluid injection. J. Geophys. Res., **119**, 1008-1019.

Okada, Y. (1985) Surface deformation due to shear and tensile faults in a half-space. Bull. Seism. Soc. Am., **75**, 1435-1154.

Twiss, R., and E. Moores (2007), Structural geology. 2 ed.: W.H. Freeman and Company.

Zoback, M.D and Gorelick, S.M, (2012), Earthquake triggering and large-scale geologic storage of carbon dioxide. Proc. Natl. Acad. Sci. U.S.A., **109**, 5185–5189.

Zoback, M. D., (2010), Reservoir Geomechanics. Cambridge University Press.